Communications in Physics, Vol. 32, No. 1 (2022), pp. 29-37
DOI: https://doi.org/10.15625/0868-3166/16920

IMPACT OF MAGNETIC FIELD ON MAGNETIC STATES IN KAGOME MAGNETS

TRAN THI THANH MAI AND TRAN MINH TIEN†

Institute of Physics, Vietnam Academy of Science and Technology, Hanoi, Vietnam

E-mail: †minhtien@iop.vast.vn

Received 31 December 2021; *Accepted for publication 18 March 2022*
Published 25 March 2022

Abstract. *Impact of magnetic field on the magnetic states in kagome magnets is studied. The magnetic field is patterned in such a way that it can generally maintain the most prominent magnetic states in kagome magnets, such as the out-of-plane ferromagnetism and the in-plane antiferromagnetism. The tight-binding model with the spin-orbit coupling and the magnetic field on the kagome lattice is exactly solved. In both the out-of-plane ferromagnetic and the in-plane antiferromagnetic states the magnetic field opens a gap at half filling. In the out-of-plane ferromagnetic state both the half topological state, where only one spin component is topologically nontrivial, and the quantum spin anomalous Hall effect, where both spin components are topologically nontrivial, can be observed. The in-plane antiferromagnetic state may be insulating, but it is topologically trivial. The quantum anomalous Hall effect may also be observed in canted* $\sqrt{3} \times \sqrt{3}$ *antiferromagnetic state.*

Keywords: kagome lattice, spin-orbit coupling, topology, electron correlation.

Classification numbers: 71.27.+a,71.30.+h, 75.10.-b, 73.43.Nq.

I. INTRODUCTION

Kagome magnets are magnetic materials, the lattice structure of which is based on the kagome lattice [1, 2]. The kagome lattice is a two-dimensional lattice of sharing triangles (see Fig. 1). Although the kagome magnets are three dimensional, they are usually layered with principal layers of two-dimensional kagome lattice. Studies suggested that the essential properties of kagome magnets can be understood within the two-dimensional layer of kagome lattice [1, 2]. Due to the special feature of the lattice geometry, the kagome lattice exhibits a geometric frustration. Various magnetic states may exist in kagome magnets [1, 2]. Recently, experiments observed a magnetic competition between the out-of-plane ferromagnetism (FM) and the in-plane antiferromagnetism (AFM) in the kagome magnets [3, 4]. In addition, the band structure of the

©2022 Vietnam Academy of Science and Technology

tight-binding model on the kagome lattice also exhibits flat-band and Dirac cone features [5]. It can potentially host nontrivial topological properties [6, 7]. Therefore, kagome magnets are an ideal host for studying the rich interplay between geometry, correlation and topology. Recently, a minimal model was proposed for the kagome magnets [8]. It describes a system of coupled itinerant electrons and magnetic impurities in a kagome lattice. The dynamics of itinerant electrons is described by a tight-binding model in the presence of spin-orbit coupling (SOC). Magnetic impurities are coupled through an anisotropic Heisenberg exchange. Itinerant electron and magnetic impurities are coupled via an anisotropic Hund coupling. Variational calculations indeed revealed the magnetic competition between the out-of-plane FM and the in-plane AFM [8]. The anisotropic Heisenberg exchange can drive the magnetic phase transition between the out-of-plane FM and the in-plane AFM. The Hund coupling generates double exchange processes between itinerant electrons, thus magnetic ordering of itinerant electrons also simultaneously occurs with the ordering of magnetic impuritiers. Although the minimal model can qualitatively explains various observed properties of kagome magnets, it is still complicated, and cannot be solved exactly. Alternatively, we can simplify the proposed model by eliminating magnetic impurities. Actually, in kagome magnets the magnetization is intrinsic due to electron correlations [3, 4]. The magnetization impacts on itinerant electrons like an external magnetic field. Therefore, instead of magnetic impurities, we include a magnetic field in the tight-binding model of itinerant electrons. The pattern of magnetic field is selected in such a way that it can mimic and maintain the magnetic state of kagome magnets. In contrast to the minimal model, the simplified model can exactly be solved. It also allows us to study the impact of magnetic field (or magnetization) on electrons in magnetic states in a simple way. Because, kagome magnets are candidates for observing the quantum (spin) anomalous Hall effect (Q(S)AHE), the edge modes and the Hall conductivity in the simplified model can predict the possible existence of the QAHE or QSAHE in certain conditions, and this would help both theoretical and experimental investigations in searching the QAHE and the QSAHE. In particular, we also find a half topological out-of-plane FM state, where only one spin component is topologically nontrivial.

The rest of the present paper is organized as follows. In Sec. II we propose the simplified model, which can describe magnetic states in kagome magnets. The numerical results are presented in Sec. III. Finally, Sec. IV is the conclusion.

II. MODEL

We consider a single system of electrons in the presence of magnetic field. Its Hamiltonian can be written as follows

$$H = -t\sum_{\langle i,j\rangle,\sigma} c^{\dagger}_{i\sigma}c_{j\sigma} - i\lambda\sum_{\langle i,j\rangle,\sigma} \nu_{ij}c^{\dagger}_{i\sigma}\sigma c_{j\sigma} - \sum_{i,ss'}\mathbf{h}_i\cdot c^{\dagger}_{is}\boldsymbol{\sigma}_{ss'}c_{is'}. \quad (1)$$

The first term in Hamiltonian (1) describes the electron hopping in the kagome lattice. The hopping parameter is t. i, j are the lattice sites, and the symbol $\langle i,j\rangle$ denotes the nearest-neighbor sites. $c^{\dagger}_{i\sigma}$ ($c_{i\sigma}$) is the creation (annihilation) operator for electron with spin σ at lattice site i. The second term in Hamiltonian (1) is the SOC of electrons. The SOC is realized through the direction-dependent hopping with the parameter λ and the sign $\nu_{ij} = \pm 1$ as shown in Fig. 1. The last term of Hamiltonian (1) describe an external magnetic field. The magnetic field $\mathbf{h}_i$ applies to electrons

at lattice site i, and is patterned by the magnetic configuration of the magnetic states in kagome magnets.

The hopping and the SOC terms can be combined into a single complex hopping

$$-t\sum_{\langle i,j\rangle,\sigma} c^{\dagger}_{i\sigma}c_{j\sigma} - i\lambda\sum_{\langle i,j\rangle,\sigma} \nu_{ij}c^{\dagger}_{i\sigma}\sigma c_{j\sigma} = -\sum_{\langle i,j\rangle,\sigma} t_{\sigma}c^{\dagger}_{i\sigma}c_{j\sigma}, \tag{2}$$

where $t_{\sigma} = t \pm i\sigma\lambda$. The $\pm$ sign depends on the hopping direction as shown in Fig. 1. Because the hopping parameter is complex, it can be presented as $t_{\sigma} = re^{\pm i\sigma\Phi/3}$, where $r = \sqrt{t^2+\lambda^2}$, and $\Phi = 3\arg(t+i\lambda)$. r and $\Phi/3$ are the modulus and the argument of the complex number $t+i\lambda$. The parameter r can be interpreted as an effective hopping magnitude in the presence of SOC. The parameter Φ is equivalent to a magnetic flux which penetrates each triangle of the kagome lattice. When an electron hops round a triangle, it attains a Peierls phase, which equals to the flux Φ, penetrating the triangle. The Peierls phase is an effect of the SOC on the electron hopping in the kagome lattice. The SOC is the key ingredient for maintaining non-trivial topology of the ground state [9–11]. In the presence of magnetic ordering, it interplays with the magnetization and may give rise to the QAHE [12, 13]. In the following we use $r = 1$ as the energy unit.

Although the magnetic field is external, it can be considered as an intrinsic effect of long-range magnetic ordering. For instance, when the Hund coupling between electrons and magnetic impurities is present, the molecular mean field generated from the Hund coupling can play as a magnetic field [8]. Because in kagome magnets various magnetic states occur, and they can be maintained by the magnetic field. The most prominent magnetic states in kagome magnets are out-of-plane FM and in-plane AFM [1–4]. In the out-of-plane FM state, the local magnetization at each lattice site is parallel to the z axis. In the in-plane AFM state, the local magnetizations completely lie in the xy plane, and their directions form 120° angle from each other, as depicted

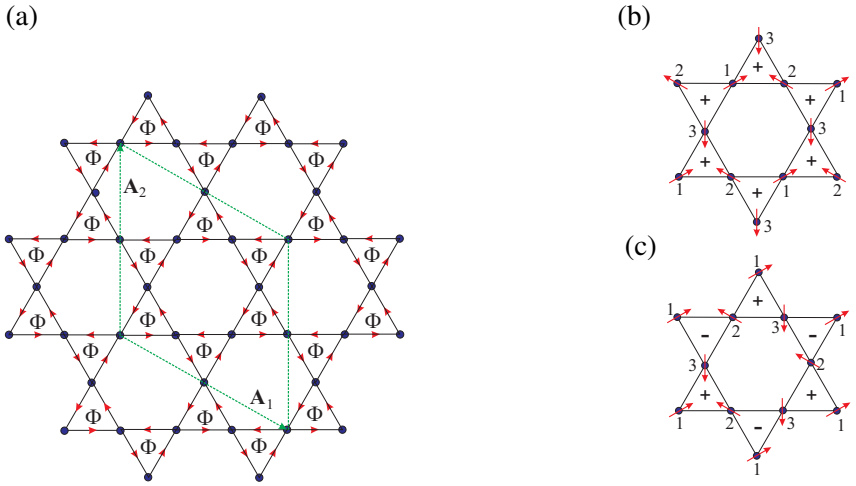

Fig. 1. (a) Lattice structure of kagome lattice. The arrows on lattice edges denote the sign $\nu_{ij} = 1$ of the SOC. Φ is the flux penetrating each triangle. The dotted rhombus is the $\sqrt{3}\times\sqrt{3}$ unit cell with the basis vectors $\mathbf{A}_1$, $\mathbf{A}_2$. The lattice parameter between the nearest-neighbor sites $a = 1$. (b) & (c) In-plane 1×1 and $\sqrt{3}\times\sqrt{3}$ AFM states with the spin chirality $\chi = \pm 1$, respectively. The indices $1, 2, 3$ denote the pattern of the magnetic field for the in-plane AFM states.

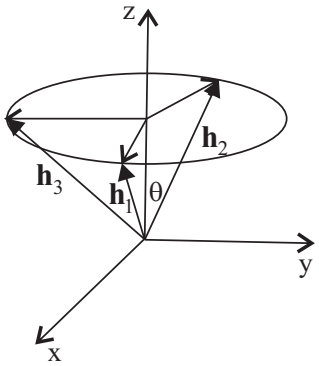

Fig. 2. Sketch of magnetic field which maintains the canted AFM state. Its projection in the *xy* plane forms the 120° AFM state.

in Fig. 1. There are two different in-plane AFM states. They are distinguishable by the vector chirality for three spins locating in each triangle of the kagome lattice [14]

$$\boldsymbol{\chi} = \frac{2}{3\sqrt{3}} \sum_{(i\neq j)=1,2,3} \mathbf{S}_i \times \mathbf{S}_j, \tag{3}$$

where $\mathbf{S}_i$ is ordered spin at lattice i, and it is normalized $|\mathbf{S}_i| = 1$. For the in-plane states the vector chirality directs to the z axis and it can be reduced to its magnitude χ, defined by $\boldsymbol{\chi} = \chi \mathbf{e}_z$, where $\mathbf{e}_z$ is the unit vector in the z axis. The 1×1 and $\sqrt{3}\times\sqrt{3}$ in-plane AFMs are characterized by the uniform ($\chi = 1$) and staggered chirality ($\chi = \pm 1$), as shown in Fig. 1. The minimal unit cell, which can describe both the 1×1 and $\sqrt{3}\times\sqrt{3}$ in-plane AFMs, is the $\sqrt{3}\times\sqrt{3}$ unit cell, as depicted in Fig. 1. For maintaining the out-of-plane FM and the 1×1 (or $\sqrt{3}\times\sqrt{3}$) in-plane AFM, the pattern of magnetic field can be based on the configuration of magnetic field at the three sites of a triangle of the kagome lattice, as shown in Fig. 1. In general, it can be presented as following

$$\mathbf{h}_1 = (-M\frac{\sqrt{3}}{2}\sin\theta, -M\frac{1}{2}\sin\theta, M\cos\theta), \tag{4}$$

$$\mathbf{h}_2 = (M\frac{\sqrt{3}}{2}\sin\theta, -M\frac{1}{2}\sin\theta, M\cos\theta), \tag{5}$$

$$\mathbf{h}_3 = (0, M\sin\theta, M\cos\theta), \tag{6}$$

where θ is the polar angle of the magnetic field $\mathbf{h}_i$ at site i of the triangle ($i = 1,2,3$). M is the magnitude of the magnetic field $|\mathbf{h}_i| = M$ ($i = 1,2,3$). Actually, the magnetic field generally maintains the canted magnetic state, where the projection of the magnetization in the *xy*-plane forms the 120° AFM state, as sketched in Fig. 2. When $\theta = 0$ the magnetic state is actually reduced to the out-of-plane FM state, where the magnetization is parallel the z-axis. When $\theta = \pi/2$, the magnetic state is the in-plane AFM. Therefore the above pattern of magnetic field is suitable for studying the impact of magnetic field on both the out-of-plane FM and the in-plane AFM states. It is similar to the molecular mean field generated from the Hund and Heisenberg exchange

couplings [8]. The out-of-plane FM and the in-plane AFM states were indeed observed in the kagome magnets [1–4].

Hamiltonian (1) can exactly be solved. It is actually quadratic. Indeed, we can rewrite Hamiltonian in the following form

$$H = \sum_{I,J,a,b,s,s'} c^\dagger_{Ias} E_{as,bs'}(I,J) c_{Jbs'}, \tag{7}$$

where I, J are the indices of unit cells, and a, b are the indices of the lattice sites within the unit cells. s, s' are the spin indices. Suppose the kagome lattice consists of N unit cells, and each unit cell contains N_c lattice sites. For the $\sqrt{3}\times\sqrt{3}$ unit cell, $N_c = 9$. The matrix $E_{as,bs'}(I,J)$ is

$$E_{as,bs'}(I,J) = t_{abs}(I,J)\delta_{ss'} - h_{Ia}\delta_{IJ}\delta_{ab}\sigma_{ss'}, \tag{8}$$

where $t_{abs}(I,J) = -t_s$ when lattice sites Ia and Jb are nearest neighbor, and $t_{abs}(I,J) = 0$ otherwise. Using the Fourier tranform

$$c_{\mathbf{k}as} = \frac{1}{\sqrt{N}} \sum_I c_{Ias} e^{i\mathbf{R}_I\cdot\mathbf{k}}, \tag{9}$$

where $\mathbf{R}_I$ is the position of unit cell I, we obtain

$$H = \sum_{\mathbf{k}} \hat{C}^\dagger_{\mathbf{k}} \hat{E}(\mathbf{k}) \hat{C}_{\mathbf{k}}, \tag{10}$$

where $\hat{C}^\dagger_{\mathbf{k}} = (c^\dagger_{\mathbf{k}1\uparrow}\cdots c^\dagger_{\mathbf{k}N_c\uparrow} c^\dagger_{\mathbf{k}1\downarrow}\cdots c^\dagger_{\mathbf{k}N_c\downarrow})$, and

$$E_{as,bs'}(\mathbf{k}) = \frac{1}{N}\sum_{I,J} E_{as,bs'}(I,J) e^{-i(\mathbf{R}_I-\mathbf{R}_J)\cdot\mathbf{k}}.$$

The matrix $\hat{E}(\mathbf{k})$ can be diagonalized, and its eigenvalues are the electron spectra of the system. When the eigenvalues and the eigenvectors of $\hat{E}(\mathbf{k})$ are obtained, we can compute the electron filling as well as other physical quantities. In particular, the Hall conductivity can be calculated by the Kubo formula [8, 15]

$$\sigma_{xy} = \frac{e^2}{2\pi}\frac{1}{N}\sum_{\mathbf{k},n,m} \frac{\mathrm{Im}[\langle\mathbf{k}n|j_x|\mathbf{k}m\rangle\langle\mathbf{k}m|j_y|\mathbf{k}n\rangle]}{(\mathscr{E}_{\mathbf{k}n}-\mathscr{E}_{\mathbf{k}m})^2}(f(\mathscr{E}_{\mathbf{k}n}) - f(\mathscr{E}_{\mathbf{k}m})), \tag{11}$$

where e is the electric charge of electron, j_α is the current operator in α-direction, $|\mathbf{k}n\rangle$ and $\mathscr{E}_{\mathbf{k}n}$ are the normalized eigenstate and eigenvalue of $\hat{E}(\mathbf{k})$, $f(x) = 1/(\exp(x/T)+1)$ is the Fermi-Dirac distribution function at temperature T. The current operator can be determined by

$$\mathbf{j} = i[H,\mathbf{P}], \tag{12}$$

where $\mathbf{P} = \sum_{Ias}\mathbf{r}_{Ia}c^\dagger_{Ias}c_{Ias}$ is the polarization operator, and $\mathbf{r}_{Ia}$ is the position of lattice site Ia [15].

III. NUMERICAL RESULTS

In this section we present the numerical results at zero temperature. In Fig. 3 we plot the dependence of filling on the chemical potential and the magnitude of the magnetic field for various canted angles. We focus on the insulating state because the QAHE can only occur in the insulating state. When the electron filling does not change with increasing chemical potential, the state is insulating. In the color plot in Fig. 3 it corresponds to the region of constant color. Without the magnetic field ($M = 0$), the insulating state only appears at filling $2/3$ and $4/3$. One

can notice that the magnetic field mixes electrons with different spins, therefore the spin index is no longer a good quantum number, except for the case $\theta = 0$. Figure 3 shows that the magnetic field opens a gap at half filling. It gradually increases the gap, especially in the in-plane AFM state. However, in the out-of-plane FM state, the opened gap does not linearly depend on the magnitude of magnetic field. The SOC usually also opens a gap, for example in the honeycomb lattice [9]. When the magnetic field is present, both the magnetic field and the SOC together open the gap at half filling [12]. However, in the kagome lattice the SOC opens a gap only at fillings $2/3$ and $4/3$ [5]. At half filling, only the magnetic field can open the gap. This implies that in the kagome lattice, the magnetic field and the SOC separately induce the insulating state at different fillings.

The edge states can be detected from the spectra of a nanoribon which is cut from the kagome lattice. For simplicity, we cut the kagome lattice along the basis vectors $\mathbf{A}_1 = (3/2, -\sqrt{3}/2)$, $\mathbf{A}_2 = (0, \sqrt{3})$ of the $\sqrt{3} \times \sqrt{3}$ unit cell. The periodic boundary condition is set along the $\mathbf{A}_1$ direction. In numerical calculations we take 10 unit cells along the $\mathbf{A}_2$ direction. In Fig. 4 we plot the spectra of the nanoribon in the canted 1×1 and $\sqrt{3} \times \sqrt{3}$ AFM states at a fixed magnitude M. Figure 4 shows that the spectra do not have the particle-hole symmetry. Indeed, in contrast to the honeycomb lattice, in the kagome lattice the tight-binding model lacks the particle-hole symmetry [5]. Therefore, in the kagome lattice the electron and hole dopings are not equivalent. Figure 4 also shows that the gap is opened at half filling in both the canted 1×1 and $\sqrt{3} \times \sqrt{3}$ AFM states. However, the gap decreases with the canted angle θ in the canted $\sqrt{3} \times \sqrt{3}$ AFM state, but with larger magnetic field magnitude, the gap is still opened in the in-plane $\sqrt{3} \times \sqrt{3}$ AFM state ($\theta = \pi/2$). At half filling the conducting edge states appear in the out-of-plane FM

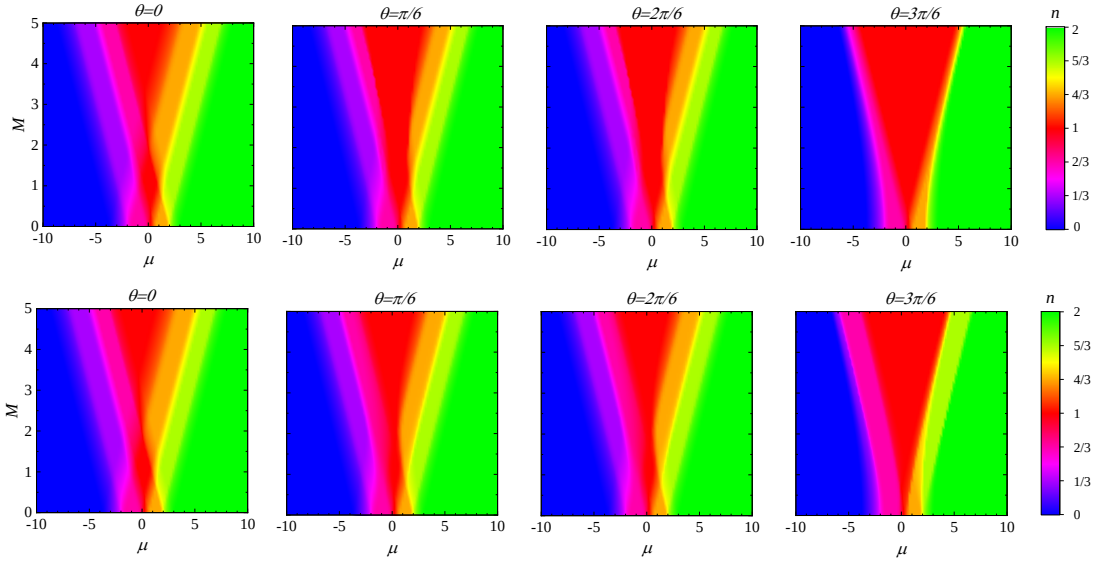

Fig. 3. (Color online) Color plot of electron filling via the chemical potential μ and the magnitude of the magnetic field M for various canted angles θ. Upper (lower) row plots the results for the canted 1×1 ($\sqrt{3} \times \sqrt{3}$) AFM magnetic field pattern. Model parameters: $r = 1$, $\Phi = \pi/3$.

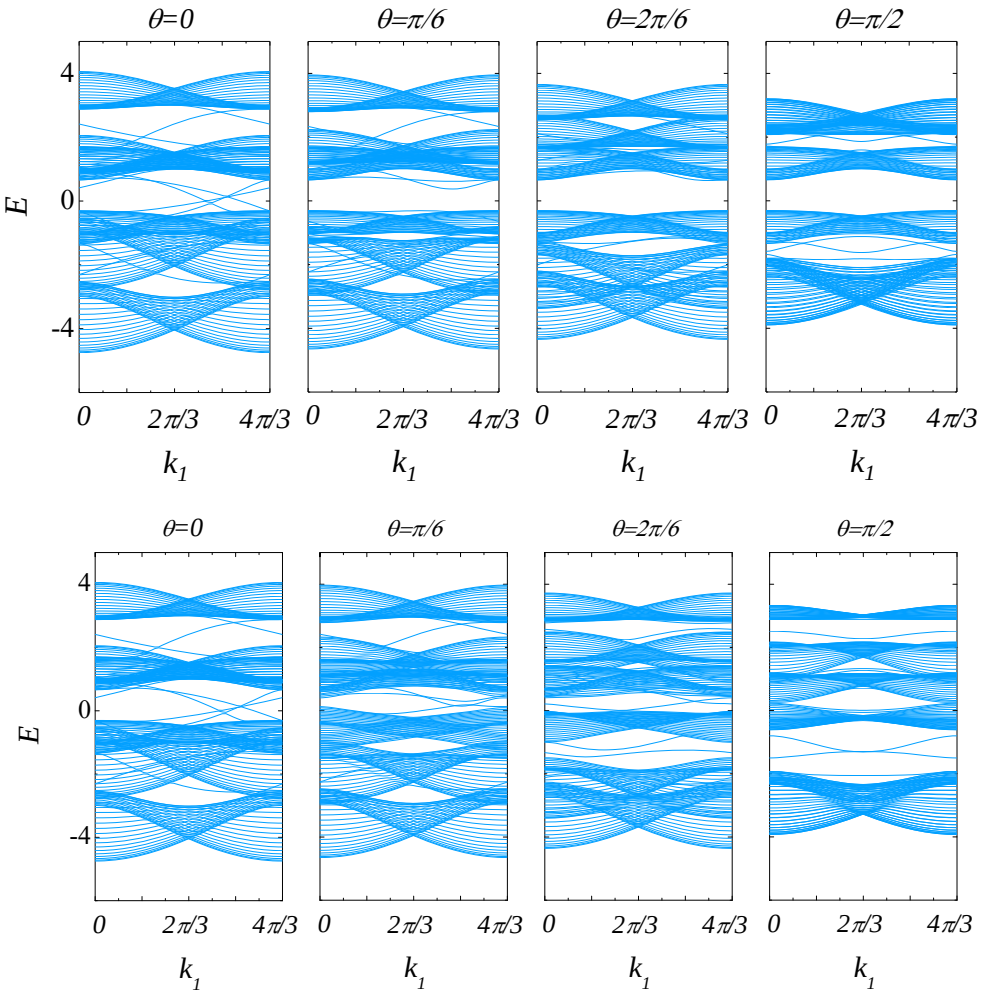

Fig. 4. (Color online) Spectra of nanoribon cut from the kagome lattice along the basis vectors $\mathbf{A}_1$ and $\mathbf{A}_2$ in the canted AFM state at fixed $M = 1$. Upper (lower) row plots the spectra in the canted 1×1 ($\sqrt{3} \times \sqrt{3}$) AFM states. Model parameters: $r = 1$, $\Phi = \pi/3$.

state ($\theta = 0$). In this case ($\theta = 0$), spin is a good quantum number, therefore we can analyze the Hall conductivity for each spin component. In Fig. 5 we plot the Hall conductivity for spin up and down components as a function of the magnitude of magnetic field. It shows that the Hall conductivity is quantized $\sigma_{xy} = \sigma$ for spin component σ when $M_{1\sigma} \leq M \leq M_{2\sigma}$. Numerical calculations reveal $M_{i\uparrow} < M_{i\downarrow}$ ($i = 1, 2$), therefore there are 3 distinguishable topological regimes. When $M < M_{1\uparrow}$ or $M > M_{2\downarrow}$, both spin components are topologically trivial. When $M_{1\uparrow} \leq M < M_{1\downarrow}$ or $M_{2\uparrow} < M \leq M_{2\downarrow}$, one spin component is topologically nontrivial, while the other spin component is topologically trivial. We refer this state as half topological. The half topological state was previously found in an AFM state [16, 17]. Our finding shows that it can also occur in a FM or

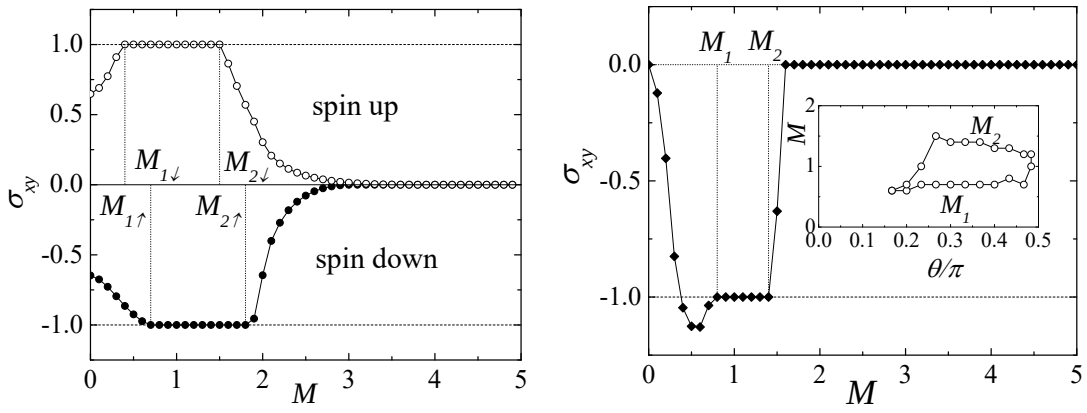

Fig. 5. The Hall conductivity in unit $e^2/2\pi$ as a function of the magnitude M of magnetic field at half filling. Left panel: in the out-of-plane FM state ($\theta = 0$). Right panel: in the canted $\sqrt{3}\times\sqrt{3}$ AFM state ($\theta = 2\pi/6$). The insert plots the phase diagram of topologically nontrivial canted $\sqrt{3}\times\sqrt{3}$ AFM state. Model parameters: $r = 1$, $\Phi = \pi/3$.

ferrimagnetic state. When $M_{1\downarrow} \le M \le M_{2\uparrow}$, the Hall conductivity for both spin components are quantized. However, the charge Hall conductivity vanishes, and only the spin Hall conductivity is quantized. This implies that at half filling the QSAHE can be observed in the out-of-plane FM state. When $\theta \neq 0$, spin is no longer a good quantum number, and we cannot analyze the ground state properties by the spin orientation. However, in the canted 1×1 AFM states ($\theta \neq 0$), numerical calculations reveal that the charge Hall conductivity vanishes at half filling. This is consistent with the absence of the edge states in the canted 1×1 AFM state at half filling as shown in Fig. 4. In Fig. 5 we also plot the Hall conductivity in the canted $\sqrt{3}\times\sqrt{3}$ AFM state at half filling. It also shows that the Hall conductivity is quantized when $M_1 \le M \le M_2$. This is consistent with the appearance of the edge state in the canted $\sqrt{3}\times\sqrt{3}$ AFM state at half filling as shown in Fig. 4. The phase diagram of the QAHE is also presented in Fig. 5. The QAHE occupies in a finite region of M and θ. Note that the in-plane AFM state ($\theta = \pi/2$) may be insulating, but it is topologically trivial.

IV. CONCLUSION

We have studied the impact of magnetic field on the magnetic states in kagome magnets. The magnetic field maintains the magnetic states and it can open a gap at half filling. The gap gradually increases with the magnitude of magnetic field in the in-plane AFM state, but does not linearly depend on the magnetic field in the out-of-plane FM state. We use both the edge states and the Hall conductivity to identify topologically nontrivial states. The numerical results reveal that the QSAHE and half topological states can occur in the half filling out-of-plane FM state. In half filling the canted 1×1 AFM states are topologically trivial. However, the $\sqrt{3}\times\sqrt{3}$ AFM state may exhibit the QAHE at half filling in a finite region of the canted angle and of the magnitude of magnetic field. However, the in-plane AFM state is topologically trivial.

ACKNOWLEDGEMENT

This research is funded by Vietnam National Foundation for Science and Technology Development (NAFOSTED) under Grant No 103.01-2019.309.

REFERENCES

[1] J-X. Yin, S. Pan and M.Z. Hasan, *Probing topological quantum matter with scanning tunnelling microscopy*, *Nat. Rev. Phys.* **3** (2021) 249.

[2] M. Z. Hasan, G. Chang, I. Belopolski, G. Bian, S.-Y. Xu and J.-X. Yin, *Weyl, Dirac and high-fold chiral fermions in topological quantum matter*, *Nat. Rev. Mat.* **6** (2021) 784.

[3] Z. Guguchia, J. A. T. Verezhak, D. J. Gawryluk, S. S. Tsirkin, J.-X. Yin, I. Belopolski, H. Zhou, G. Simutis, S.-S. Zhang, T. A. Cochran, G. Chang, E. Pomjakushina, L. Keller, Z. Skrzeczkowska, Q. Wang, H. C. Lei, R. Khasanov, A. Amato, S. Jia, T. Neupert, H. Luetkens and M. Z. Hasan, *Tunable anomalous Hall conductivity through volume-wise magnetic competition in a topological kagome magnet*, *Nat. Commun.* **11** (2020) 559.

[4] Z. Guguchia, H. Zhou, C. N. Wang, J. X. Yin, C. Mielke, S. S. Tsirkin, I. Belopolski, S. S. Zhang, T. A. Cochran, T. Neupert, R. Khasanov, A. Amato, S. Jia, M. Z. Hasan and H. Luetkens, *Multiple quantum phase transitions of different nature in the topological kagome magnet* $Co_3\ Sn_{2-x}\ In_xS_2$, *npj Quantum Materials* **6** (2021) 50.

[5] K. Ohgushi, S. Murakami and N. Nagaosa, *Spin anisotropy and quantum Hall effect in the kagomé lattice: Chiral spin state based on a ferromagnet*, *Phys. Rev. B* **62** (2000) R6065.

[6] E. Liu, Y. Sun, N. Kumar, L. Muechler, A. Sun, L. Jiao, S.-Y. Yang, D. Liu, A. Liang, Q. Xu, J. Kroder, V. Süß, H. Borrmann, C. Shekhar, Z. Wang, C. Xi, W. Wang, W. Schnelle, S. Wirth, Y. Chen, S. T. B. Goennenwein and C. Felser, *Giant anomalous Hall effect in a ferromagnetic kagome-lattice semimetal*, *Nat. Phys.* **14** (2018) 1125.

[7] Q. Wang, Y. Xu, R. Lou, Z. Liu, M. Li, Y. Huang, D. Shen, H. Weng, S. Wang and H. Lei, *Large intrinsic anomalous Hall effect in half-metallic ferromagnet* $Co_3Sn_2S_2$ *with magnetic Weyl fermions Nat. Commun.* **9** (2018) 3681.

[8] Thanh-Mai Thi Tran, Duong-Bo Nguyen, Hong-Son Nguyen and Minh-Tien Tran, *Magnetic competition in topological kagome magnets*, *Mater. Res. Express* **8** (2021) 126101.

[9] C. L. Kane and E. J. Mele, *Quantum spin hall effect in graphene*, *Phys. Rev. Lett.* **95** (2005) 226801.

[10] C. Weeks and M. Franz, *Topological insulators on the Lieb and perovskite lattices*, *Phys. Rev. B* **82** (2010) 085310.

[11] C. Weeks and M. Franz, *Flat bands with nontrivial topology in three dimensions*, *Phys. Rev. B* **85** (2012) 041104.

[12] Minh-Tien Tran, Hong-Son Nguyen and Duc-Anh Le, *Emergence of magnetic topological states in topological insulators doped with magnetic impurities*, *Phys. Rev. B* **93** (2016) 155160.

[13] Thanh-Mai Thi Tran, Duc-Anh Le, Tuan-Minh Pham, Kim-Thanh Thi Nguyen, Minh-Tien Tran, *Phys. Rev. B* **102** (2020) 205124.

[14] D. Grohol, K. Matan, J. H. Cho, S. H. Lee, J. W. Lynn, D. G. Nocera and Y. S. Lee, *Spin chirality on a two-dimensional frustrated lattice*, *Nat. Mat.* **4** (2005) 323.

[15] G. D. Mahan, *Many-Particle Physics*, 3rd edition (Plenum publisher, 2000).

[16] Minh-Tien Tran, Duong-Bo Nguyen, Hong-Son Nguyen, and Thanh-Mai Thi Tran, Topological Green function of interacting systems, arXiv:2104.02344 [cond-mat.str-el].

[17] T. I. Vanhala, T. Siro, L. Liang, M. Troyer, A. Harju, and P. Törmä, *Topological phase transitions in the repulsively interacting haldane-hubbard model*, *Phys. Rev. Lett.* **116** (2016) 225305.